

Article

Heat Triggered Release Behavior of Eugenol from Tobacco Leaf

Xuyang Song ¹, Min Wei ^{1,*}, Xi Pan ¹, Yunlu He ¹, Xinjiao Cui ², Xiaodi Du ^{2,*} and Junsheng Li ^{2,*} 

¹ Technology Centre of Hubei China Tobacco Industry Co., Ltd., Wuhan 430051, China; songxy@hbtobacco.cn (X.S.); 11013210@hbtobacco.cn (X.P.); heyunlu@hbtobacco.cn (Y.H.)

² School of Chemistry, Chemical Engineering and Life Sciences, Wuhan University of Technology, Wuhan 430070, China; 304805@whut.edu.cn

* Correspondence: weimin@hbtobacco.cn (M.W.); duxiaodi@msn.com (X.D.); li_j@whut.edu.cn (J.L.)

Abstract: Fragrance is a commonly used substance in a number of commercial products, and fine control over the release behavior of the fragrance is essential for its successful application. Understanding the release behavior of the fragrance is the key to realizing the control of its release. Herein, we use tobacco leaf as the model substrate and investigate the mechanism of eugenol release from tobacco leaf. Our results show that interaction between eugenol and tobacco leaf is weak physical adsorption, and the eugenol release from tobacco leaf substrate is a temperature-dependent process. Further analysis on the release behavior reveals that eugenol release is closely associated with the morphology change of tobacco leaves under heating conditions. Our results provide insight into the release mechanism of fragrance from polymer substrate and may be useful for the future design of fragrance release systems.

Keywords: fragrance release; heat triggered; mechanism; diffusion



Citation: Song, X.; Wei, M.; Pan, X.; He, Y.; Cui, X.; Du, X.; Li, J. Heat Triggered Release Behavior of Eugenol from Tobacco Leaf. *Appl. Sci.* **2021**, *11*, 8642. <https://doi.org/10.3390/app11188642>

Academic Editors:
Wojciech Kolanowski and
Anna Gramza-Michałowska

Received: 12 August 2021
Accepted: 15 September 2021
Published: 17 September 2021

Publisher's Note: MDPI stays neutral with regard to jurisdictional claims in published maps and institutional affiliations.



Copyright: © 2021 by the authors. Licensee MDPI, Basel, Switzerland. This article is an open access article distributed under the terms and conditions of the Creative Commons Attribution (CC BY) license (<https://creativecommons.org/licenses/by/4.0/>).

1. Introduction

Fragrance can bring a pleasant scent or help to shield unwanted smells. Therefore, fragrances are widely used in a variety of commercial products ranging from consumable commodities to industrial goods. The volatile nature of a typical fragrance is the premise for its function to deliver the characteristic pleasant scent. However, the volatile nature of fragrance also leads to the gradual decay of its scent. From the point of practical application, it is important to prolong the release period of the fragrance [1–4].

A common approach to prolong the release period of fragrance is to immobilize the fragrance onto an appropriate carrier [5–9]. Polymer carriers, particularly edible polymers, have been widely used to stabilize fragrance. For example, menthol loaded on a sorbitan monostearate carrier can be stabilized for at least 15 days under ambient conditions [10]. In comparison, pristine menthol lost 62.1% of its initial weight under identical conditions after 15 days. In general, the carrier should have good compatibility with the fragrance to ensure homogeneous dispersion of fragrance within the carrier. In addition, the affinity between the carrier and the fragrance should be designed to achieve both high stability of fragrance under storage conditions and desirable release behavior under working conditions. Furthermore, the carrier materials are preferably biocompatible and free of odor. Due to the constraints above, it is tricky to design a fragrance carrier.

Direct loading of the fragrance onto the substrate material of the product is simple and more cost-effective than the use of fragrance carriers. However, it is challenging to achieve precise control over the release behavior of the fragrance on such a release system. This is because that the interaction between the fragrance and substrate involves a series of complex interactions such as intra-molecular interactions and steric hindrance [11–13]. Understanding the interactions between the fragrance and substrate on both the microscopic and macroscopic levels is key to the rational design of fragrance release systems. Herein, we use eugenol as the model fragrance and tobacco leaf as the substrate and investigate

the release mechanism of eugenol from tobacco leaf. The observed release behavior is correlated with the microscopic interactions between eugenol and tobacco leaf.

2. Materials and Methods

2.1. Materials

Isopropanol (99.7 wt%), ethanol (99.8 wt%), naphthalene (99.0 wt%), eugenol (98.0 wt%) and Whatman Cambridge filters were purchased from Alladin Reagent Co., Ltd. Heat-not-burn cigarettes were supplied by China Tobacco Hubei Co., Ltd.

2.2. Loading of Eugenol

Eugenol was dissolved in the ethanol solution to prepare the eugenol solution for fragrance loading (10 wt%). The solution was injected into the tobacco leaf of cigarettes with a syringe. The amount of eugenol injected into each cigarette was controlled to be 0.5% of the mass of the tobacco leaf.

2.3. Eugenol Release Experiment

The release of eugenol from the tobacco leaf was quantified with a self-made cigarette smoking device (Figure 1). The released eugenol was captured with a Whatman Cambridge filter for subsequent quantification. The release experiments were initiated after the heating chamber was heated to 220 °C, 230 °C, 240 °C, 250 °C and 260 °C, respectively. The suction interval was 30 s, and the suction duration was 2 s. Each suction volume was 55 mL, and a total of 8 aspirations were taken.

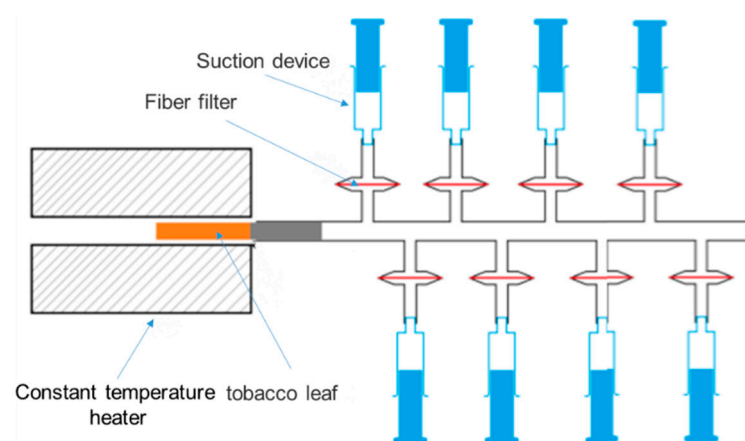


Figure 1. The self-made fragrance release analysis system.

2.4. Quantitative Analysis Experiment

The filters with released eugenol were put into the sample bottles, and 20 mL of isopropanol solution with standard internal naphthalene was added. The mixed solution was shaken at room temperature for 60 min. The supernatant was collected after centrifugation and then used for chromatographic determination.

The GC conditions were as follows: DB-FFAP capillary column (30 m × 0.53 mm × 0.25 μm) was set at 80 °C for 1 min, then the column temperature was raised to 220 °C at a rate of 10 °C min⁻¹ for 9 min. The inlet temperature was 220 °C, the split ratio was 2:1, the carrier gas was H₂, and the column flow rate was 8 mL min⁻¹. The sampling volume was 1 μL. The temperature of the FID detector was set to 260 °C. For accurate quantitative analysis, 2 mg L⁻¹, 4 mg L⁻¹, 6 mg L⁻¹, 8 mg L⁻¹, 10 mg L⁻¹ eugenol standard solution containing standard internal naphthalene was prepared, respectively, and the standard curve was determined.

2.5. Characterization

FTIR measurement: First, a drop of eugenol was dropped on the surface of the tobacco leaf. After volatilization for a period of time, absorbable cotton was used to absorb the excess eugenol on the surface of the tobacco leaf. The sample was detected by a VATAR FT-IR370 spectrometer. The wavelength range is 400–4000 cm^{-1} .

Thermal stability analysis. The thermal stability of eugenol, tobacco and eugenol-loaded tobacco leaf was tested by STA449F3/STA449F3 thermal analyzer under the following conditions: N_2 atmosphere, room temperature to 500 $^\circ\text{C}$, heating rate 10 $^\circ\text{C min}^{-1}$.

SEM (scanning electron microscope) characterization: a JSM-7500F/JSM-7500F scanning electron microscope was used to photograph the morphology of unheated tobacco and heated tobacco at 220 $^\circ\text{C}$, 250 $^\circ\text{C}$ and 260 $^\circ\text{C}$, respectively.

DFT (density function theory) analysis: all structural optimization and energy calculations were conducted using the Materials Studio's DMOL 3 module. The generalized gradient approximation method (GGA)-Perdew-Burke-Ernzerhof (PBE) functional was used to calculate the exchange-correlation energy. The basis set was double numerical orbital Basis set + orbital polarization function (DNP). In order to accelerate the iterative convergence rate of the SCF, orbit relaxation was allowed in the calculation process, and the Fermi Smearing value was set as 0.005 ha. The convergence criteria for energy change, max force and atomic displacement were set to 1×10^{-5} Ha, 2×10^{-3} Ha \AA^{-1} and 5×10^{-3} \AA , respectively. After the convergence test, the accuracy of the Orbital Cut-off was set as 4.9 \AA , and the calculation formula of binding energy (E_b) was calculated according to the following equation:

$$E_b = E_{\text{total}} - E_G - E_C$$

where E_{total} , E_G and E_C represent the total energy after combination and the monomer energy after structural optimization, respectively.

3. Results

Eugenol, giving out the odor of cloves, is a commonly used fragrance with weak acidity. Eugenol was selected as the model fragrance for this investigation due to its importance in food chemistry. Eugenol was loaded onto commercial tobacco leaf by injection of the eugenol solution onto the tobacco leaf. The amount of loaded eugenol was controlled to be 0.005 mg mg^{-1} in all experiments. Successful loading of eugenol on tobacco leaf was demonstrated with FT-IR measurements. Tobacco leaf is a complex mixture mainly composed of cellulose, monosaccharide, starch, lignin, etc. A group of characteristic vibration peaks from these main components were clearly observed in the FT-IR spectra of tobacco leaf. For example, peaks associated with stretching vibrations of the C=O group in the acetyl group of cellulose, stretching vibration of the phenyl group in lignin and stretching vibration of C=O group in aryl ether compounds of lignin were observed at 1737, 1543 and 1240 cm^{-1} [14,15], respectively. Other characteristic peaks of tobacco leaf were also labeled in Figure 2. In the FT-IR spectra of eugenol, peaks from the stretching vibration of C-O in -OCH (1428 cm^{-1}), stretching vibration of -C-O (1261 cm^{-1}) and in-plane wagging vibration of phenyl hydroxyl groups (1235 cm^{-1}) could be identified. These characteristic peaks of eugenol were also observed in the spectra of eugenol-loaded tobacco leaf, suggesting successful loading of eugenol onto the tobacco leaf. Next, the interaction of eugenol with the tobacco leaf was investigated with theoretical calculations. Since the main component of tobacco leaf is cellulose (~6–25%), monosaccharides (e.g., glucose, ~10–25%), starch (~10–30%) and lignin (~1–13%), the adsorption configurations of eugenol on these components were calculated to give an insight into the adsorption mechanism of eugenol on a tobacco leaf. The optimized molecular configuration of the adsorption is shown in Figure 3. The adsorption energy of eugenol on cellulose, monosaccharide (D-glucose), starch and lignin was calculated to be -0.06, -0.125, -0.202 and -0.288 eV, respectively. The negative adsorption energy suggests that the eugenol adsorption on tobacco leaf is thermodynamically favorable. In addition, the low adsorption energy indicates that the adsorption of eugenol on tobacco leaves is weak physical adsorption.

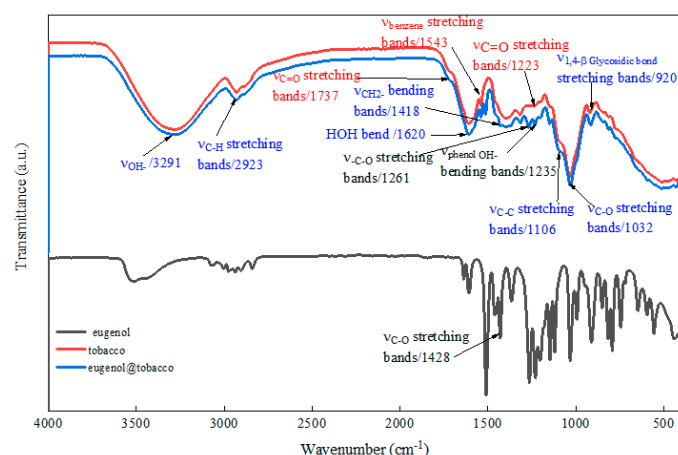


Figure 2. FTIR spectra of eugenol, tobacco leaf and tobacco leaf loaded with eugenol.

The thermal stability of eugenol, tobacco and eugenol-loaded tobacco leaf was evaluated with thermogravimetry (TG) analysis in argon (Figure 4). The tobacco leaf exhibited a four-stage weight loss. At a temperature below 130 °C (state I), the weight loss mainly resulted from the loss of physically adsorbed water and volatile species in the sample. In the temperature range of 150 to 270 °C (stage II), the weight loss of tobacco leaf was largely from the heat-induced release of glycerol (a common additive in tobacco leaf), nicotine and initial decomposition of cellulose and lignin. Further increases in the temperature led to the thermolysis and carbonization of cellulose and lignin, which caused rapid weight loss (stage IV). As a volatile solution, eugenol evaporated quickly as temperature increased. Eugenol completely evaporated at 220 °C. Compared with pristine tobacco leaf, tobacco leaf loaded with eugenol experienced a faster weight loss with temperature increase due to the incorporation of eugenol. The TG results above show the release of eugenol at a high rate above 200 °C. Considering that the working temperature of the fragrance release system in heat, not burn, cigarettes is normally between 200 °C to 260 °C, the release of eugenol from tobacco leaf loaded with eugenol was investigated in this temperature range. The released eugenol was collected sequentially (time interval 30 s) at eight different spots of the sampling chamber. The amount of collected eugenol was quantified with GC analysis. The eugenol release experiment was repeated for three times at each heating temperature, and the average value was taken as the release amount at the sampling point after quantification.

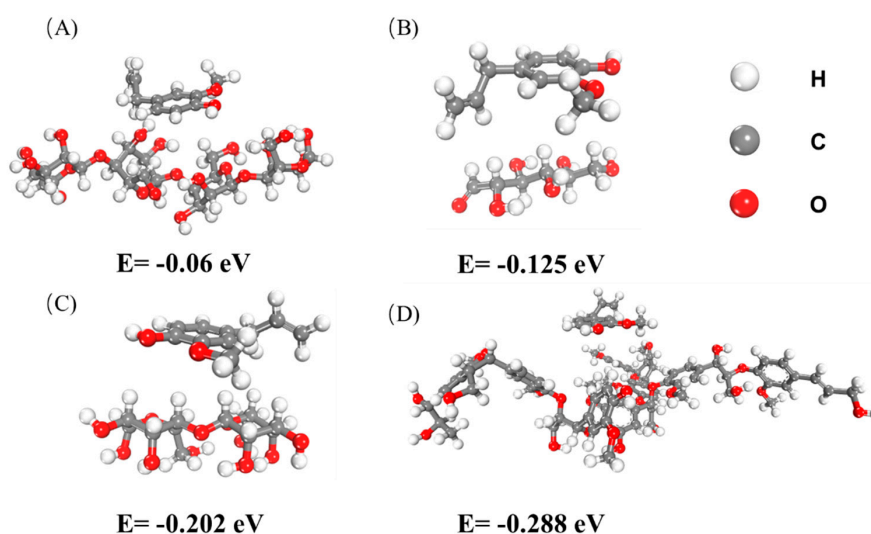


Figure 3. Optimized configuration showing the adsorption of eugenol on (A) cellulose, (B) monosaccharide, (C) starch and (D) lignin.

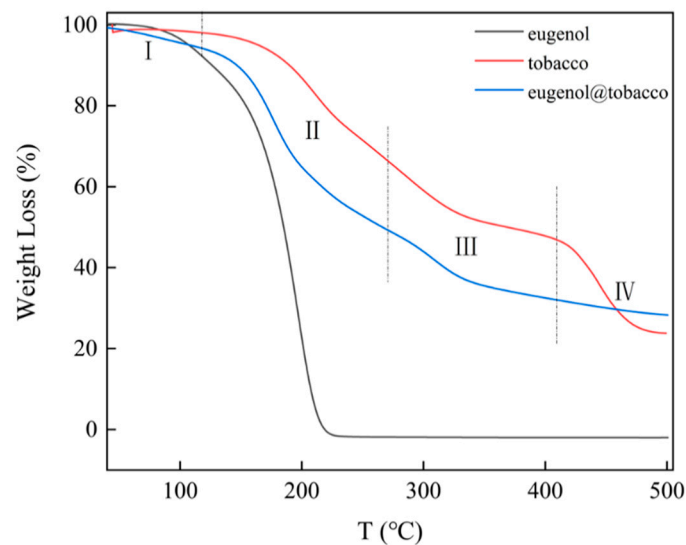


Figure 4. Thermal gravity analysis of eugenol, tobacco and tobacco leaf loaded with eugenol.

According to the results above, the time-dependent release behavior of eugenol from tobacco can be plotted (Figure 5). Generally, the eugenol release amount firstly increased and then decreased with time. For example, the released eugenol was 7.89, 12.07, 13.69, 12.60, 10.65, 9.64, 9.37 and 8.76 μg at 32, 64, 96, 128, 160, 192, 224 and 256 s, respectively at a heating temperature of 260 $^{\circ}\text{C}$. From the comparison of the release profiles collected at different temperatures, it was observed that the amount of released eugenol increased with heating temperature until 250 $^{\circ}\text{C}$. When the heating temperature increased to 260 $^{\circ}\text{C}$, the amount of released eugenol dropped quickly. Depending on the state of the tobacco leaf substrate, the release of eugenol can follow a Fick or non-Fick process.

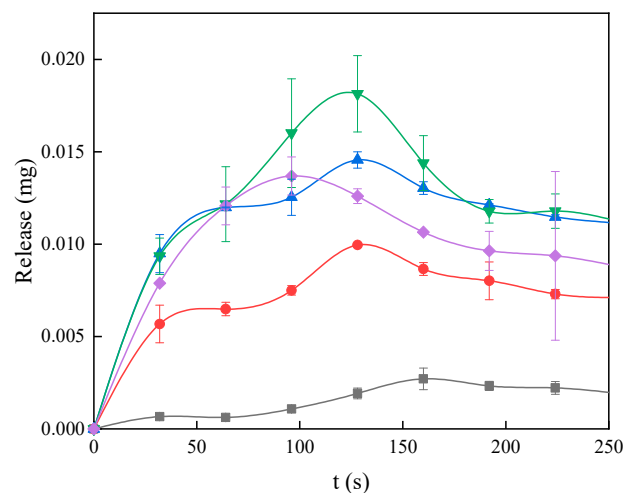


Figure 5. The time-lapse release behavior of eugenol from tobacco leaf (the error bar represents the standard deviation of the measured value from three individual experiments).

To further understand the changes in the release behavior of eugenol at different temperatures, SEM images of the pristine tobacco leaf and tobacco leaf after release experiments were collected and compared. It was seen that the pristine tobacco leaf had a smooth surface morphology with micro-sized particles ($\sim 20 \mu\text{m}$) scattered on the surface of the tobacco leaf (Figure 6A). The surface morphology of tobacco leaves after heating at 220 $^{\circ}\text{C}$ and 250 $^{\circ}\text{C}$ remained similar (Figure 6B,C). In contrast, the microparticles on the tobacco leaf after release experiments at 260 $^{\circ}\text{C}$ showed slit pores on the surface (outlined with red circles, Figure 6D). The emergence of these pores could be caused by the internal

stress due to an abrupt increase in the heat release of additives from the internal tobacco leaf at 260 °C. The increased release of tobacco leaf additives and the changes in tobacco leaf morphology could be key factors that influence the release of eugenol at 260 °C.

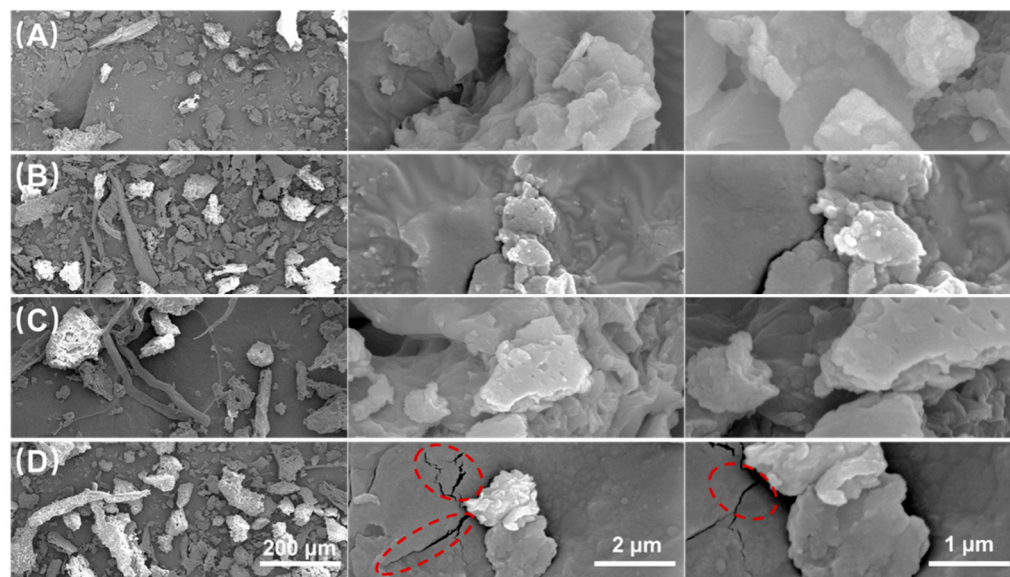


Figure 6. SEM images of (A) pristine tobacco leaf and tobacco leaf after eugenol release experiments conducted at (B) 220 °C, (C) 250 °C and (D) 260 °C.

4. Conclusions

A model fragrance release system with eugenol as the fragrance and tobacco leaf as the substrate was studied in detail. Theoretical DFT studies reveal that the adsorption of eugenol on tobacco leaves is weak physical adsorption. Such weak physical adsorption makes the thermally triggered release of eugenol possible. Experimental analysis of the release behavior showed that the morphology change of tobacco leaf induced by heating could be a key factor influencing the release behavior. The theoretical insight gained in this study may provide a useful guide for the rational design of fragrance release systems.

Author Contributions: Conceptualization, J.L.; methodology, X.C. and X.D.; investigation, X.S., M.W., X.P. and Y.H.; writing—review and editing, X.C. and J.L.; supervision, J.L.; project administration, M.W. All authors have read and agreed to the published version of the manuscript.

Funding: This research was funded by Hubei China Tobacco Industry Co., LTD. (2021JCXL2JS2A001).

Institutional Review Board Statement: No study involving humans or animals is conducted in this work.

Informed Consent Statement: Informed consent was obtained from all subjects involved in the study.

Data Availability Statement: Data is available on request to corresponding author.

Conflicts of Interest: The authors declare no conflict of interest.

References

1. Wei, M.; Pan, X.; Rong, L.; Dong, A.; He, Y.; Song, X.; Li, J. Polymer carriers for controlled fragrance release. *Mater. Res. Express* **2020**, *7*, 082001. [[CrossRef](#)]
2. Chakraborty, S. Carrageenan for encapsulation and immobilization of flavor, fragrance, probiotics, and enzymes: A review. *J. Carbohydr. Chem.* **2017**, *36*, 1–19. [[CrossRef](#)]
3. Liu, L.; Chen, G.; Fishman, M.L.; Hicks, K.B. Pectin gel vehicles for controlled fragrance delivery. *Drug Deliv.* **2005**, *12*, 149–157. [[CrossRef](#)] [[PubMed](#)]
4. Popadyuk, N.; Popadyuk, A.; Kohut, A.; Voronov, A. Thermoresponsive latexes for fragrance encapsulation and release. *Int. J. Cosmet. Sci.* **2016**, *38*, 139–147. [[CrossRef](#)]

5. Elesini, U.S.; Švarc, J.; Šumiga, B.; Urbas, R. Melamine formaldehyde microcapsules with fragrance core material: Preparation, properties, and end use. *Text. Res. J.* **2016**, *87*, 2435–2448. [[CrossRef](#)]
6. Liu, Y.; Wang, Y.; Huang, J.; Zhou, Z.; Zhao, D.; Jiang, L.; Shen, Y. Encapsulation and controlled release of fragrances from functionalized porous metal-organic frameworks. *AIChE J.* **2019**, *65*, 491–499. [[CrossRef](#)]
7. Seemork, J.; Tree-Udom, T.; Wanichwecharungruang, S. A refillable fragrance carrier with a tuneable thermal switch. *Flavour Fragr. J.* **2012**, *27*, 386–392. [[CrossRef](#)]
8. Xiao, Z.; Tian, T.; Hu, J.; Wang, M.; Zhou, R. Preparation and characterization of chitosan nanoparticles as the delivery system for tuberose fragrance. *Flavour Fragr. J.* **2014**, *29*, 22–34. [[CrossRef](#)]
9. Zhang, Y.; Song, J.; Chen, H. Preparation of polyacrylate/paraffin microcapsules and its application in prolonged release of fragrance. *J. Appl. Polym. Sci.* **2016**, *133*. [[CrossRef](#)]
10. Wei, M.; Song, X.; Pan, X.; Li, R.; Chen, C.; Du, X.; Li, J. Thermal Triggered Release of Menthol from Different Carriers: A Comparative Study. *Appl. Sci.* **2020**, *10*, 1677. [[CrossRef](#)]
11. Chen, H.; Chen, H.; Zhang, B.; Jiang, L.; Shen, Y.; Fu, E.; Zhao, D.; Zhou, Z. Tuning the release rate of volatile molecules by pore surface engineering in metal-organic frameworks. *Chin. Chem. Lett.* **2021**, *32*, 1988–1992. [[CrossRef](#)]
12. Li, Z.; Huang, J.; Ye, L.; Lv, Y.; Zhou, Z.; Shen, Y.; He, Y.; Jiang, L. Encapsulation of Highly Volatile Fragrances in Y Zeolites for Sustained Release: Experimental and Theoretical Studies. *ACS Omega* **2020**, *5*, 31925–31935. [[CrossRef](#)] [[PubMed](#)]
13. Kuhnt, T.; Herrmann, A.; Benczédi, D.; Weder, C.; Foster, E.J. Controlled fragrance release from galactose-based pro-fragrances. *RSC Adv.* **2014**, *4*, 50882–50890. [[CrossRef](#)]
14. Mondragon, G.; Fernandes, S.; Retegi, A.; Peña, C.; Algar, I.; Eceiza, A.; Arbelaz, A. A common strategy to extracting cellulose nanoentities from different plants. *Ind. Crops Prod.* **2014**, *55*, 140–148. [[CrossRef](#)]
15. Oh, S.Y.; Yoo, D.I.; Shin, Y.; Kim, H.C.; Kim, H.Y.; Chung, Y.S.; Park, W.H.; Youk, J.H. Crystalline structure analysis of cellulose treated with sodium hydroxide and carbon dioxide by means of X-ray diffraction and FTIR spectroscopy. *Carbohydr. Res.* **2005**, *340*, 2376–2391. [[CrossRef](#)] [[PubMed](#)]